

Disorder-induced structural transitions in topological insulating Ge-Sb-Te compounds

Jeongwoo Kim and Seung-Hoon Jhi

Citation: *Journal of Applied Physics* **117**, 195701 (2015); doi: 10.1063/1.4921294

View online: <http://dx.doi.org/10.1063/1.4921294>

View Table of Contents: <http://scitation.aip.org/content/aip/journal/jap/117/19?ver=pdfcov>

Published by the [AIP Publishing](#)

Articles you may be interested in

Structural, dynamical, and electronic properties of transition metal-doped Ge₂Sb₂Te₅ phase-change materials simulated by ab initio molecular dynamics

Appl. Phys. Lett. **101**, 024106 (2012); 10.1063/1.4736577

The origin of the resistance change in GeSbTe films

Appl. Phys. Lett. **97**, 152113 (2010); 10.1063/1.3499751

Thermal characterization of the SiO₂ - Ge₂Sb₂Te₅ interface from room temperature up to 400 °C

J. Appl. Phys. **107**, 044314 (2010); 10.1063/1.3284084

Thickness and stoichiometry dependence of the thermal conductivity of GeSbTe films

Appl. Phys. Lett. **91**, 111904 (2007); 10.1063/1.2784169

Phase change behaviors of Sn-doped Ge-Sb-Te material

Appl. Phys. Lett. **90**, 091904 (2007); 10.1063/1.2475390

A promotional banner for AIP Applied Physics Reviews. The background is a dark blue gradient with a bright light source on the right, creating a lens flare effect. On the left, there is a small image of a journal cover titled 'AIP Applied Physics Reviews' showing a 3D lattice structure. The main text 'NEW Special Topic Sections' is in large, white, bold font. Below it, 'NOW ONLINE' is in yellow, followed by 'Lithium Niobate Properties and Applications: Reviews of Emerging Trends' in white. The AIP Applied Physics Reviews logo is in the bottom right corner.

NEW Special Topic Sections

NOW ONLINE
Lithium Niobate Properties and Applications:
Reviews of Emerging Trends

AIP Applied Physics
Reviews

Disorder-induced structural transitions in topological insulating Ge-Sb-Te compounds

Jeongwoo Kim and Seung-Hoon Jhi^{a)}

Department of Physics, Pohang University of Science and Technology, Pohang 790-784, Republic of Korea

(Received 25 February 2015; accepted 7 May 2015; published online 18 May 2015)

The mechanism for the fast switching between amorphous, metastable, and crystalline structures in chalcogenide phase-change materials has been a long-standing puzzle. Based on first-principles calculations, we study the atomic and electronic properties of metastable $\text{Ge}_2\text{Sb}_2\text{Te}_5$ and investigate the atomic disorder to understand the transition between crystalline hexagonal and cubic structures. In addition, we study the topological insulating property embedded in these compounds and its evolution upon structural changes and atomic disorder. We also discuss the role of the surface-like states arising from the topological insulating property in the metal-insulator transition observed in the hexagonal structure. © 2015 AIP Publishing LLC. [<http://dx.doi.org/10.1063/1.4921294>]

I. INTRODUCTION

Chalcogen-based phase-change materials (PCMs), such as Ge-Sb-Te (GST) compounds, have possible applications as non-volatile memory devices.¹ PCMs utilize the large contrast in electrical resistivity and optical reflectivity between amorphous and crystalline phases to express the binary states, and can switch between them in extremely short times (\sim nanoseconds).^{2,3} PCM is also usable in display devices that combine distinct variation of optical and electrical properties.⁴ GST compounds are pseudo-binary alloys of GeTe and Sb_2Te_3 that have an energy gap of 0.55 and 0.28 eV, respectively.^{5,6} GeTe is an ordinary band insulator whereas Sb_2Te_3 is a topological insulator.⁷ First-principles calculations show that crystalline GST compounds can also have a topological insulating phase depending on the composition and layer stacking sequence.^{8–10} Experimental observation of weak antilocalization in GeSb_2Te_4 , angle-resolved photoemission study for $\text{Ge}_2\text{Sb}_2\text{Te}_5$ (GST225), and large magneto-resistance in interfacial PCMs supports these theoretical predictions.^{11–13}

GST225 undergoes a series of structural transitions from amorphous to metastable rock-salt structure (or cubic) at $\sim 150^\circ\text{C}$ and then to stable hexagonal structure at $>300^\circ\text{C}$.¹⁴ For the hexagonal structure, three types of layer sequencing have been suggested: Petrov sequence Te-Sb-Te-Ge-Te-Ge-Te-Sb-,¹⁵ Kooi and De Hosson (KH) sequence Te-Ge-Te-Sb-Te-Te-Sb-Ge-,¹⁶ and intermixed sequence Te-Ge/Sb-Te-Te-Sb/Ge-.¹⁷ According to first-principles calculations, the KH sequence is slightly more stable than the Petrov and intermixed sequences.¹⁸ Also the superlattice of $(\text{GeTe})_m(\text{Sb}_2\text{Te}_3)_n$ with the KH sequence can be formed to release the strain energy in the hexagonal structure.¹⁹ For the cubic structure, the common belief is that 4(a) sites are solely occupied by Te and 4(b) sites by Ge, Sb, and 20% of vacancies at random.²⁰ However, first-principles calculations^{18,19} suggested that ordering in the cations and vacancy layers in

the rock-salt structure may lead to more stable structures than the fully random structure, although these calculations did not consider thermal energy and configurational entropy. Another important question is how the ordering (or disorder in cations including vacancies) affects the electronic²¹ and topological insulating property of cubic GST, especially when the spin-orbit coupling is included. Understanding the fast amorphous-crystalline transition, improving switching speed of the device, lowering the operating voltage, and exploring new types of applications all require detailed atomic and electronic structures of the rock-salt structure.

In this work, we used first-principles calculations to investigate the stability of GST225 when atomic disorder is imposed, and the structural characteristics of the metastable cubic phase. In particular, we studied the electronic structure, optimized atomic structure, and the topological insulating property of model cubic GST225 in the presence of cationic disorder. We also suggested a model transition-path for the structural transition from cubic to hexagonal structures, and accompanying changes in the electronic property.

II. COMPUTATIONAL METHODS

Our calculations were based on the density-functional theory using the projected augmented plane-wave method (PAW)^{22,23} as implemented in the Vienna *ab initio* simulation package.²⁴ The interaction between the valence electrons and ions is treated using a PAW-based pseudopotential method. The valence electron configurations are $4s^24p^2$ for Ge, $5s^25p^3$ for Sb, and $5s^25p^4$ for Te. The generalized gradient approximation (GGA) of Perdew-Burke-Ernzerhof type was used to describe the exchange-correlation of electrons.²⁵ To supplement the van der Waals (vdW) interaction between weakly bonded layers, which is not properly represented by GGA, we used the Tkatchenko and Scheffler (TS) method.²⁶ Lattice constants calculated using the TS method ($a = 4.24$; $c = 17.12 \text{ \AA}$) agree well with experimental values ($a = 4.22$; $c = 17.18 \text{ \AA}$).¹⁴ The spin-orbit coupling was included in the self-consistent calculation level. The cut-off energy for the plane-wave-basis expansion was set to 400 eV. The system

^{a)}Author to whom correspondence should be addressed. Electronic mail: jhish@postech.ac.kr

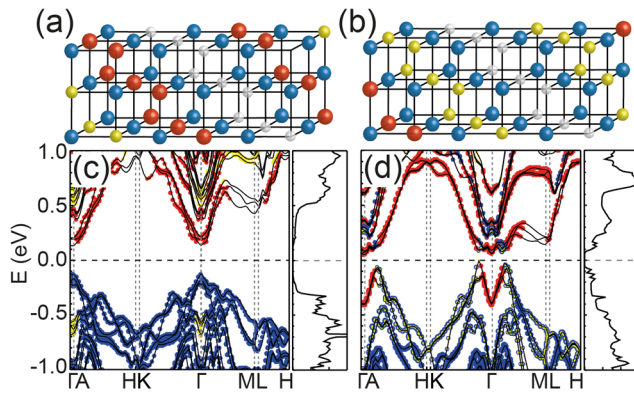


FIG. 1. Model atomic structure of $\text{Ge}_2\text{Sb}_2\text{Te}_5$ in the rock-salt structure having (a) the KH sequence and (b) the Petrov sequence along the (111) direction. Blue, Te; yellow, Ge; red, Sb; white, cation vacancies. Ge planes in the KH sequence are equivalent to Sb planes in the Petrov sequence. Calculated band structures and the density of states for the (c) KH and (d) Petrov sequences. Colored dots indicate the dominant atomic character of the states near the Fermi level. Blue, Te; yellow, Ge; red, Sb. The Fermi level is set at zero energy.

size (the number of atoms in the unit cell) and the k-point grids for the Brillouin zone integration were chosen as follows; 27 atoms and $4 \times 4 \times 1$ for the ordered cubic GST225 with KH or Petrov sequence (Fig. 1), 108 atoms and $5 \times 5 \times 2$ for the Ge-Sb exchange process from KH to Petrov sequence (Fig. 2), 243 atoms and $6 \times 6 \times 3$ for the model cubic structure with three types of disorder (Figs. 3 and 4), and 162 atoms and $12 \times 12 \times 3$ for the hexagonal structures (Fig. 5). Atomic relaxation was conducted until the change in the total energy was <0.1 meV. The parity-check method by Fu and Kane²⁷ was also used to calculate the topological invariants. To estimate the configurational entropy for GST compounds, we used the Ising model and the Boltzmann's entropy equation ($S = k_b \ln W$) where k_b is the Boltzmann constant, and $W = N!/(n_{vac}!n_{cat}!)$ is the number of microstates, with all available 4(b) sites N and two different particle occupation conditions, i.e., vacancy n_{vac} and cation sites n_{cat} . We used the Mercury program to emulate the X-ray diffraction profile for cubic GST with defects.²⁸

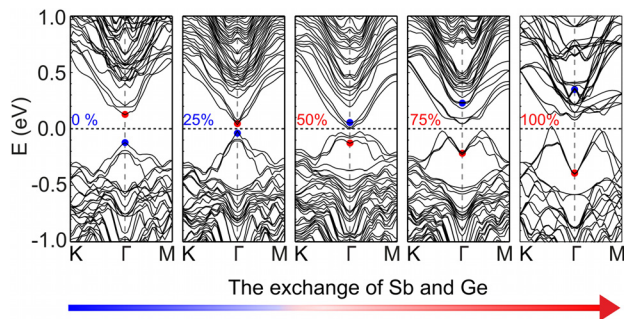


FIG. 2. Calculated band structures of GST225 in the cubic structure with a short-period superlattice order of cations along the (111) direction. From the left to the right panels, the band structures with Ge and Sb atoms exchanged by the percentage ratio starting from the KH sequence. To minimize the structural instability, the cation sites are selected so that cations do not neighbor each other. We observe a gradual decrease in the band gap and a band inversion as the exchange ratio increases. GST225 turns into a topological insulator when the exchange ratio is $\sim 50\%$. Blue dots: odd parity of the wave-function, red dots: even parity of the wave-function.

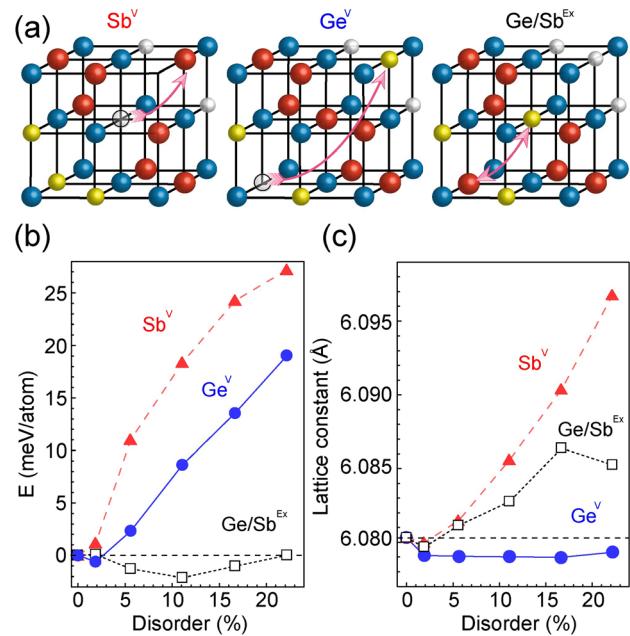


FIG. 3. (a) Schematic drawing of three types of atomic disorder in metastable GST; Sb or Ge migration to vacancy site (Sb^V , Ge^V) and the exchange of Ge and Sb (Ge/Sb^{Ex}). Red, Sb; blue, Te; yellow, Ge; white, vacancy. (b) and (c), Effect of atomic disorder on structural stability and the lattice constant, respectively, as a function of the disorder ratio.

III. RESULT AND DISCUSSION

The steady change without noticeable features in resistance during the structural transition upon heating hints at the existence of intermediate structures in GST that have characteristics of both conventional hexagonal and rock-salt structures.²⁹ We chose an initial structure of GST225 that maintains the cubic lattice with a short-period stacking order along the (111) direction (Figs. 1(a) and 1(b)). The low energy states near the Fermi level depend on the layer sequence. The initial structure with the KH sequence has a direct band gap of ~ 0.26 eV at the Γ point, whereas the structure with the Petrov sequence has an indirect band gap of about 0.06 eV and an inverted orbital character (Figs. 1(c) and 1(d)). The large difference between electronic structures of these sequences is attributed to relatively strong hybridization of Ge and Te-Te layers in the Petrov sequence: the valence bands in the KH sequence are formed solely by non-bonding p_z orbitals of the Te layers adjacent to the vacancy layer, but the valence bands in the Petrov sequence are derived from the orbitals in both Ge and Te layers, and are consequently pushed upward in energy.

Insulating behavior of the compounds observed in experiments seems to fit better with the large energy gap of the KH sequence than with the Petrov sequence. Also, in the initial cubic structure the KH sequence is energetically more stable than the Petrov sequence by 20 meV/atom. Based on these results, we chose the KH sequence along the (111) direction in the initial cubic structure. First, we studied the effect on the electronic property of Ge-Sb exchange, which leads to a mixing of KH and Petrov sequences. As the Ge-Sb exchange ratio is increased, the conduction and valence bands move toward the Fermi level, and the band inversion

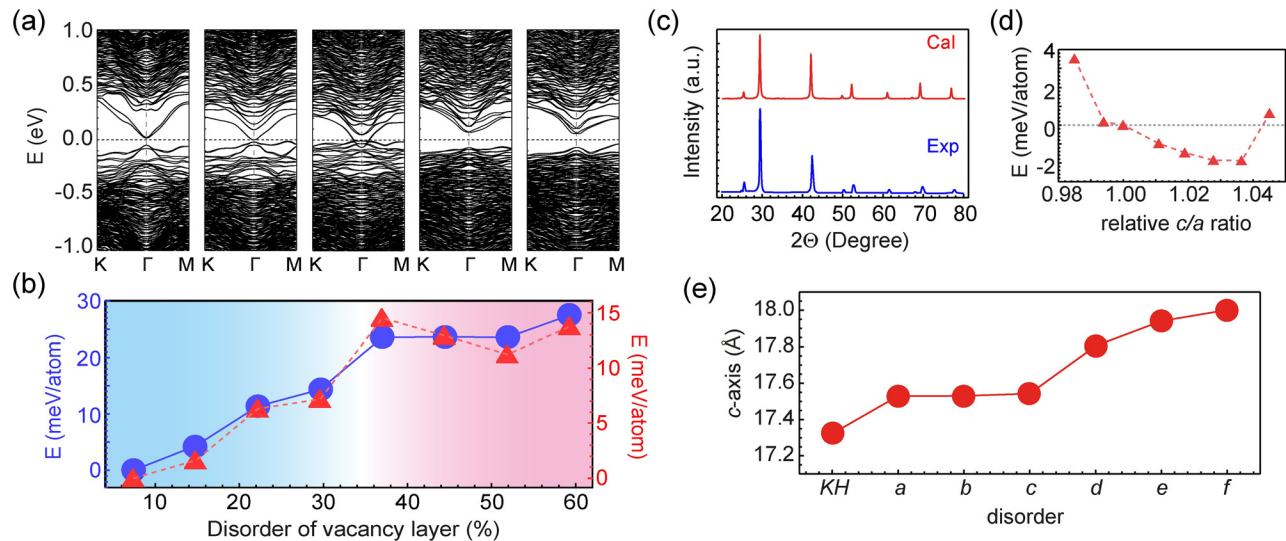


FIG. 4. (a) Calculated band structures of cubic GST with a disorder ratio of (from left to right panels) 7.4%, 14.8%, 29.6%, 37.0%, and 51.9% in the vacancy layer (b) The free energy with (red triangles, right) or without (blue dots, left) the configurational entropic term for varying disorder ratios in the vacancy layers. (c) Simulated X-ray diffraction (upper, red line) for 44.4% disorder. Lower (blue) line: the experimental data reproduced from Ref. 14. (d) Total energy for varying c/a ratio with $r_{dv} = 29.6\%$. The c/a ratio of ideal cubic structure is set to 1. (e) Calculated c -axis lattice constant of hexagonal GST225 with KH sequence as a function of degree of atomic disorder from a to f in increasing disorder ratio, 11.1% Ge/Sb^{Ex}, 16.7% Ge/Sb^{Ex}, 8.3% Ge/Sb^{Ex} + 5.5% r_{dv} , 11.1% Ge/Sb^{Ex} + 11.1% r_{dv} , 11.1% Ge/Sb^{Ex} + 22.2% r_{dv} , and 11.1% Ge/Sb^{Ex} + 33.3% r_{dv} .

occurs at the Γ point at about 1:1 exchange (50% disorder) (Fig. 2). The band inversion indicates that cubic GST225 transforms to a topological insulating phase above this exchange ratio as found in the hexagonal structure.⁸ Our calculations suggest that cationic disorder by Ge-Sb exchange affects mostly the low energy states near the Fermi level and eventually induces formation of the topological insulating phase in our cubic GST225.¹³ This trend demonstrates that the disorder not only affects the electronic band structure but also can control its topological nature. These observations in turn imply that metastable cubic GST may have different topological phases controlled by the degree of disorder, which can be exploited to realize multilevel states.^{30,31} Also, natural inhomogeneity in the distribution of defects³² may produce domains with differing topological insulating phases along which interface states can develop, thereby providing electrical conduction channels that generate Joule heating. Our findings suggest that GST can be used as fundamental structure in which the occurrence and effects of inhomogeneous topological phases in homogenous materials and associated physical properties can be studied.

Next, we investigated the atomic structure of the cations including vacancies in the 4(b) sublattice of the rock-salt structure.^{20,33} We calculated the structural stability of GST225 when three different types of atomic disorder were considered (Fig. 3(a)): migration of Sb or Ge into the vacancy sites (Sb^V or Ge^V) and the Ge-Sb exchange (Ge/Sb^{Ex}). We found that Sb/Te antisite defects are less stable (up to 17%) than the cationic defects that we consider in this study. We calculated total energies of GST225 upon introducing the atomic disorder up to a ratio of 20% relative to the ordered cubic structure with the KH sequence (Fig. 3(b)); Sb^V disorder immediately destabilized the structure but Ge^V disorder up to about 2% was energetically stable. More importantly, calculations suggest that structures that have up to 20% Ge/Sb^{Ex}

disorder are more stable and preferable than the well-ordered initial structure; this observation contradicts the conclusions of previous studies that found that ordered stacking structures are energetically more stable than intermixed structures.¹⁸ Similar results as in our study were also reported in a previous first-principles study.¹⁹ Our finding implies that metastable GST may inherently have substantial Ge/Sb^{Ex} disorder from the energetics point of view even without considering the thermal effect. In summary, our calculations indicate that a substantial amount of Ge-Sb exchange (in an order of $\sim 10\%$) and a few percent Ge migration into vacancy sites are energetically favorable in the cubic structure even without considering entropic thermal energies.

We also investigated the effect of the cationic disorder on the lattice constant (Fig. 3(c)). Due to the small atomic size of Ge, Ge^V disorder slightly decreased the lattice constant for almost all the whole range of disorder ratio r_{dv} , which is defined as the proportion of available sites in the vacancy layer that are occupied by cations. However, Sb^V migration and Ge/Sb^{Ex} increased the lattice constant significantly in proportion to r_{dv} . These results suggest that the decrease of lattice constants during heating in experiment¹⁴ is related to Sb arrangement. A previous first-principles study also shows that the lattice constants are very sensitive to the ordering in the cation layers.¹⁹

Now, to reproduce the cubic GST225 capturing experimental observations, we focus on the electronic and structural features, and energetics upon variation of the ratio of both Ge^V and Sb^V disorder. The atomic structure of the model cubic GST was selected based on our calculations of energetics for the disorder. We found that Ge tends to separate from other Ge, and that Sb tends to occupy the empty sites that are surrounded by Ge atoms in the vacancy layers. In simulations of the exchange of cations, we minimized the structural instability by choosing a disorder configuration in

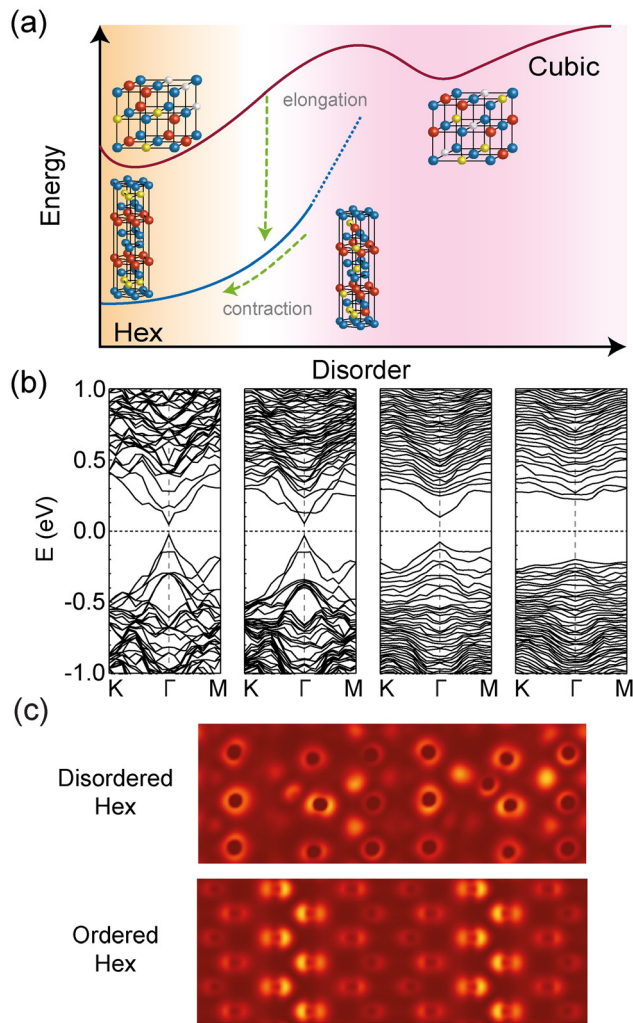


FIG. 5. (a) Schematic of hypothesized transition path of GST225 from cubic to hexagonal structures. (b) Calculated band structures of GST225 in the hexagonal structure, from left to right panels, starting from well-ordered KH sequence, with 11.1% Ge/Sb^{Ex}, 11.1% Ge/Sb^{Ex} + 11.1% r_{dv} , and 11.1% Ge/Sb^{Ex} + 22.2% r_{dv} . (c) Charge density plot of (upper panel) the disordered hexagonal (11.1% Ge/Sb^{Ex} + 22.2% r_{dv}) in the energy window from -0.35 to -0.25 eV and (lower panel) the ordered hexagonal GST225 with KH sequence in the energy window from -0.25 to the Fermi Level.

which cations were not adjacent to each other. The supercell of our model cubic structure had 243 atoms, and the ratio of Ge:Sb:Te:vacancy was exactly 2:2:5:1. We calculated band structures (Fig. 4(a)) for r_{dv} . The observed range was $7.4 \leq r_{dv} \leq 51.9\%$. When a small amount of disorder ($r_{dv} = 7.4\%$; Fig. 4(a), leftmost panel) was introduced, localized states (flat bands) appeared near the top of the valence bands; these states were driven by the disorder. The surface-like bands from Sb₂Te₃ layers, while being also affected by the defects to have a gap opening (~ 0.06 eV) and merging into bulk bands, still retain some features of linear dispersion. At $r_{dv} > 30\%$, the linear bands disappear and the band-gap at the Γ point is increased. The conduction bands mostly from Sb atoms were insensitive to cation migration to the vacancy layer but very sensitive to the Sb-Te interatomic distance. The band gap increased and the states originating from Sb orbitals became localized when Sb-Te interatomic distance was varied (e.g., in the range 2.8–3.5 Å).

Calculated total energies increased at small r_{dv} but saturated at $r_{dv} \sim 37\%$ (Fig. 4(b)). If the configurational entropic term is included, a local minimum might develop in the free energy curve. For example, at 500 K, a dip in the free energy occurred at $r_{dv} \sim 50\%$, which corresponds to the metastable cubic structure. The simulated X-ray diffraction pattern (Fig. 4(c)) for $r_{dv} \sim 50\%$ matches the peak pattern observed in experiments;¹⁴ the similarity indicates that the cubic structure in our calculations emulates successfully the metastable cubic structure. Another finding of this analysis of cationic disorder is that rearrangement of Sb and Ge into cationic layers by heating increases the c/a ratio. Calculated total energy for 29.6% r_{dv} exhibits a dip at $\sim 4\%$ elongation (Fig. 4(d)). Once transformed to the hexagonal structure, the cation ordering shrinks the c -axis (Fig. 4(e)); this change is critical in restoring the topological insulating property.⁸

Finally, we discuss a model (Fig. 5(a)) of transition path from cubic to hexagonal structures based on our calculations. As temperature is increased, Sb and Ge tend to assemble in the [111] planes, and this cation ordering (reduction in the vacancy disorder ratio) leads to contraction in lattice constants (Fig. 3(c)). In addition to the ordering in cationic planes, the vacancy layers also become ordered along the (111) direction, so the c -axis elongated in the (111) direction (Fig. 4(d)). When the ratio reaches a critical value (or cation ordering), the cubic-to-hexagonal transition occurs. In the hexagonal structure, the cationic ordering derives the c -axis contraction (Fig. 4(e)). As the cationic ordering is completed, Sb₂Te₃ layers recover the topological insulating property to generate the linear bands at the interface to GeTe layers (Fig. 5(b)). The effect of natural p -type doping by Ge-site vacancies on the electrical resistivity of GST compound increases once such linear bands are restored. The linear band dispersion with a large group-velocity provides higher carrier mobility compared with the localized band for the same amount of carrier density. Hence Ge-site vacancies³⁴ may turn the GST compounds into a metallic state more effectively with the linear bands than without them; i.e., the metal-insulator transition may be induced in the hexagonal structure by the degree of cationic ordering even in the absence of structural transition.^{14,29}

The interlayer distance is sensitive to the vdW interaction. The atomic relaxation using the TS vdW correction method leads to $\sim 3\%$ contraction of the Te-Te distance in the KH-sequence hexagonal GST, which then becomes semi-metallic. In contrast, the overall band dispersion is almost unaffected. The vdW correction may expedite the transition of hexagonal GST to a metallic phase upon the cation ordering but does not alter the trend in the electronic structures (Fig. 5). The charge-density plots of disordered hexagonal within the energy range from -0.35 to -0.25 eV and of ordered hexagonal GST225 within the energy range from -0.25 to the Fermi level (Fig. 5(c)) illustrate the change in the wave-functions upon the cation ordering. Well-localized states became extended upon the cation ordering, and this ordering may lead to the transitional behavior in the electrical conduction of GST compounds.

IV. SUMMARY

We investigated the effect of atomic disorder on structural and electronic properties in cubic GST225. Upon introducing three different types of cation disorder (Ge^{V} , Sb^{V} , and Ge/Sb^{Ex} ; Ge, Sb migration into vacancy layers and Ge-Sb exchange, respectively) into the ordered cubic GST225 with the KH sequence, we showed that Ge^{V} and Ge/Sb^{Ex} lead to a more stabilized structure and that Sb^{V} and Ge/Sb^{Ex} increase the lattice constants. We found that the topological insulating phase of GST225 also emerges as the amount of cation-exchange is increased. Emulated cubic structures with atomic disorder exhibit a dip in free energy at a disorder ratio of about 50% and reproduce the X-ray patterns of metastable cubic GST225. Based on our calculations of lattice constants and total energies, we presented a possible pathway for the transition from cubic to hexagonal structure. Upon formation of ordered cationic layers in the hexagonal structure, we showed that topological insulating property of Sb_2Te_3 layers and consequently Dirac cone-like linear bands are restored and may link to the metal-insulator transition. Our results may help to understand the mechanism by which structural and electronic transitions occur in GSTs and to explore properties that emerge due to the topological insulating nature of the compounds.

ACKNOWLEDGMENTS

This work was supported by the SRC Center for Topological Matter (No. 2011-0030789), the IT R&D program of MKE/KEIT (No. KI 10039200), and the NRL program of MOST/KOSEF (No. 2009-S001-01). This work was also supported by the Supercomputing Center/Korea Institute of Science and Technology Information with supercomputing resources including technical support (No. KSC-2013-C3-042).

¹M. Wuttig and N. Yamada, *Nat. Mater.* **6**, 824 (2007).

²S. R. Ovshinsky, *Phys. Rev. Lett.* **21**, 1450 (1968).

³M. H. R. Lankhorst, B. W. S. M. M. Ketelaars, and R. A. M. Wolters, *Nat. Mater.* **4**, 347 (2005).

⁴P. Hosseini, C. D. Wright, and H. Bhaskaran, *Nature* **511**, 206 (2014).

⁵K. Shportko, S. Kremers, M. Woda, D. Lencer, J. Robertson, and M. Wuttig, *Nat. Mater.* **7**, 653 (2008).

⁶R. Sehr and L. R. Testardi, *J. Phys. Chem. Solids* **23**, 1219 (1962).

⁷H. Zhang, C.-X. Liu, X.-L. Qi, X. Dai, Z. Fang, and S.-C. Zhang, *Nat. Phys.* **5**, 438 (2009).

⁸J. Kim, J. Kim, and S.-H. Jhi, *Phys. Rev. B* **82**, 201312(R) (2010).

⁹J. Kim, J. Kim, K.-S. Kim, and S.-H. Jhi, *Phys. Rev. Lett.* **109**, 146601 (2012).

¹⁰B. Sa, J. Zhou, Z. Sun, J. Tominaga, and R. Ahuja, *Phys. Rev. Lett.* **109**, 096802 (2012).

¹¹N. P. Breznay, H. Volker, A. Palevski, R. Mazzarello, A. Kapitulnik, and M. Wuttig, *Phys. Rev. B* **86**, 205302 (2012).

¹²J. Tominaga, R. E. Simpson, P. Fons, and A. V. Kolobov, *Appl. Phys. Lett.* **99**, 152105 (2011).

¹³C. Pauly, M. Liebmann, A. Giussani, J. Kellner, S. Just, J. Sánchez-Barriga, E. Rienks, O. Rader, R. Calarco, G. Bihlmayer, and M. Morgenstern, *Appl. Phys. Lett.* **103**, 243109 (2013).

¹⁴I. Friedrich, V. Weidenhof, W. Njoroge, P. Franz, and M. Wuttig, *J. Appl. Phys.* **87**, 4130 (2000).

¹⁵I. I. Petrov, R. M. Imamov, and Z. G. Pinsker, *Sov. Phys. Crystallogr.* **13**, 339 (1968).

¹⁶B. J. Kooi and J. T. M. De Hosson, *J. Appl. Phys.* **92**, 3584 (2002).

¹⁷T. Matsunaga, N. Yamada, and Y. Kubota, *Acta Crystallogr., Sec. B: Struct. Sci.* **60**, 685 (2004).

¹⁸Z. Sun, J. Zhou, and R. Ahuja, *Phys. Rev. Lett.* **96**, 055507 (2006).

¹⁹J. L. F. Da Silva, A. Walsh, and H. L. Lee, *Phys. Rev. B* **78**, 224111 (2008).

²⁰N. Yamada and T. Matsunaga, *J. Appl. Phys.* **88**, 7020 (2000).

²¹J.-W. Park, S. H. Eom, H. Lee, J. L. F. Da Silva, Y.-S. Kang, T.-Y. Lee, and Y. H. Khang, *Phys. Rev. B* **80**, 115209 (2009).

²²G. Kresse and D. Joubert, *Phys. Rev. B* **59**, 1758 (1999).

²³P. E. Blöchl, *Phys. Rev. B* **50**, 17953 (1994).

²⁴G. Kresse and J. Hafner, *Phys. Rev. B* **47**, 558 (1993).

²⁵J. P. Perdew, K. Burke, and M. Ernzerhof, *Phys. Rev. Lett.* **77**, 3865 (1996).

²⁶A. Tkatchenko and M. Scheffler, *Phys. Rev. Lett.* **102**, 073005 (2009).

²⁷L. Fu and C. L. Kane, *Phys. Rev. B* **76**, 045302 (2007).

²⁸C. F. Macrae, I. J. Bruno, J. A. Chisholm, P. R. Edgington, P. McCabe, E. Pidcock, L. Rodriguez-Monge, R. Taylor, J. van de Streek, and P. A. Wood, *J. Appl. Crystallogr.* **41**, 466 (2008).

²⁹T. Siegrist, P. Jost, H. Volker, M. Woda, P. Merkelbach, C. Schlockermann, and M. Wuttig, *Nat. Mater.* **10**, 202 (2011).

³⁰Y. Yin, T. Noguchi, H. Ohno, and S. Hosaka, *Appl. Phys. Lett.* **95**, 133503 (2009).

³¹G. W. Burr, M. J. Breitwisch, M. Franceschini, D. Garetto, K. Gopalakrishnan, B. Jackson, B. Kurdi, C. Lam, L. A. Lastras, A. Padilla, B. Rajendran, S. Raoux, and R. S. Shenoy, *J. Vac. Sci. Technol., B* **28**, 223 (2010).

³²X. Q. Liu, X. B. Li, L. Zhang, Y. Q. Cheng, Z. G. Yan, M. Xu, X. D. Han, S. B. Zhang, Z. Zhang, and E. Ma, *Phys. Rev. Lett.* **106**, 025501 (2011).

³³S. Sen, T. G. Edwards, J. Y. Cho, and Y. C. Joo, *Phys. Rev. Lett.* **108**, 195506 (2012).

³⁴D. Lencer, M. Salinga, and M. Wuttig, *Adv. Mater.* **23**, 2030 (2011).